Theory of Spin-Conserving Excitation of the $N - V^-$ Center in Diamond

Adam Gali,[1,2] Erik Janzén,[3] Péter Deák,[4] Georg Kresse,[5] and Efthimios Kaxiras[2]

[1]*Department of Atomic Physics, Budapest University of Technology and Economics, Budafoki út 8., H-1111, Budapest, Hungary*
[2]*Department of Physics and School of Engineering and Applied Sciences, Harvard University, Cambridge, Massachusetts 02138, USA*
[3]*Department of Physics, Chemistry and Biology, Linköping University, S-581 83 Linköping, Sweden*
[4]*Bremen Center for Computational Materials Science, Universität Bremen, Am Fallturm 1, 28359 Bremen, Germany*
[5]*Institut für Materialphysik, Universität Wien, Sensengasse 8/12, 1090 Wien, Austria*

(Received 23 March 2009; published 27 October 2009)

The negatively charged nitrogen-vacancy defect in diamond is an important atomic-scale structure that can be used as a qubit in quantum computing and as a marker in biomedical applications. Its usefulness relies on the ability to optically excite electrons between well-defined gap states, which requires a clear and detailed understanding of the relevant states and excitation processes. Here we show that by using hybrid density-functional-theory calculations in a large supercell we can reproduce the zero-phonon line and the Stokes and anti-Stokes shifts, yielding a complete picture of the spin-conserving excitation of this defect.

DOI: 10.1103/PhysRevLett.103.186404 PACS numbers: 71.15.Mb, 61.72.Bb, 71.55.Ht

Quantum computing and its many exciting applications rely on the successful realization of quantum logic bits (qubits) that can operate under practically feasible conditions. Few physical systems can meet the requirements of controlled quantum coherence and robust operational conditions. One of the most promising candidates is the negatively charged nitrogen-vacancy defect ($N - V^-$ center) in bulk diamond [1,2]: the spin state of this defect can be manipulated using excitation from the $^3A_2$ ground state to the ^3E excited state by optical absorption (Fig. 1). The main advantage of the $N - V^-$ center is that it can operate at *room temperature* as a solid state qubit [3–9]. A detailed understanding of this excitation process is crucial in the realization of qubits based on diamond. However, achieving this level of understanding stretches the capabilities of theoretical methods that are usually applied to the study of defects in solids because of the special nature of the $N - V^-$ defect. Specifically, this defect has a strongly interacting electron system with strong coupling to the ionic degrees of freedom, and its interpretation is further complicated by contradictory experimental measurements of the emission spectrum at different temperatures [2,10].

In this Letter, we report a theoretical investigation of the radiative transitions of the $N - V^-$ center using electronic structure calculations, which give a consistent and accurate account of the excitations observed and provide a plausible resolution of the experimental situation. We utilized the HSE06 screened Hartree-Fock hybrid exchange-correlation density functional [11,12] to determine the geometry and excitation energies of the $N - V^-$ center, and we compare the results to the traditional PBE [13] exchange-correlation density functional and the experimental data. We find that—while PBE underestimates the internal electronic transitions of this defect—the HSE06 functional (which reproduces the band gap of diamond within 0.5%) reproduces the zero-phonon line and the Stokes-shift within 1.5% of experiment. This result demonstrates that hybrid functionals improve not only the excitation of the extended system (gap) but also localized ones. This promises a significant advantage in defect calculations. Motivated by the success of the hybrid functional to reproduce key experimental measurements of the excitation process, we calculate an anti-Stokes shift of 0.217 eV, measured to be 0.185 eV at usual experimental conditions at low temperature [2]. From this result, we argue that the anti-Stokes shift of 0.065 eV measured at low temperature under high-energy-density laser illumination [10], is most likely due to the local heating of the sample caused by the focused laser beam.

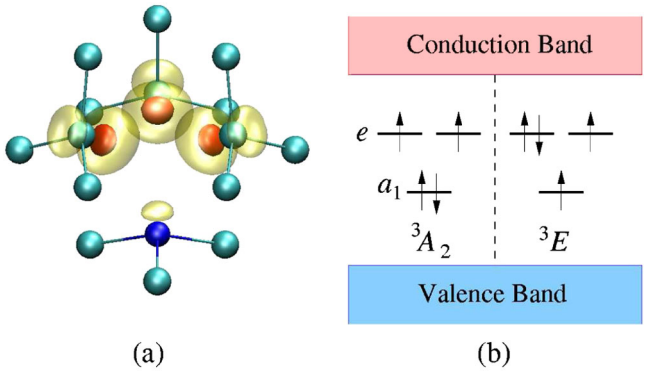

FIG. 1 (color online). (a) The structure of $N - V^-$ center in diamond; only first- and second-neighbor *C* (cyan spheres) and *N* (blue sphere) atoms to the vacant site are shown. The yellow and red lobes are contours of the calculated difference in spin density for the ^3E state as obtained by the HSE06 and PBE functionals. (b) Schematic diagram of the defect states in the gap and their occupation in the $^3A_2$ (ground) and ^3E (excited) states.

Previous density-functional-theory (DFT) calculations have shown [14–17] that in the $^3A_2$ ground state of C_{3v} symmetry the many-body wave function of this defects can be built from the single-particle band gap states: a fully occupied a_1 and a doubly degenerate e state occupied by two electrons of parallel spin. The excited ^3E state can be interpreted as promoting one electron from the a_1 single-particle level to the e level, while preserving the total spin (see Fig. 1). Our time-dependent DFT calculations on this defect in a 250-atom hydrogenated nanodiamond supports this scenario [18].

Excitation changes not only the electron wave function but the atomic structure of the defect as well. Hence, the ground state and the excited state will possess different potential energy surfaces (PES) and different vibrational states, as shown schematically in Fig. 2. The transition between the lowest PES will result in the zero-phonon line (ZPL) both in absorption and emission, a process in which no real phonons are involved in the excitation or deexcitation process. The ZPL was measured at 1.945 eV both in low-temperature absorption and emission [2]. At liquid-nitrogen temperature a broad phonon side band was measured in absorption with phonon-related peaks at approximately 2.020, 2.110, 2.180, and 2.250 eV, with the highest intensity at 2.180 eV, while in the emission band the first phonon sidebands, better resolved than in absorption, are found at 1.880, 1.820, and 1.760 eV, with the 1.760 eV peak having the highest intensity [2].

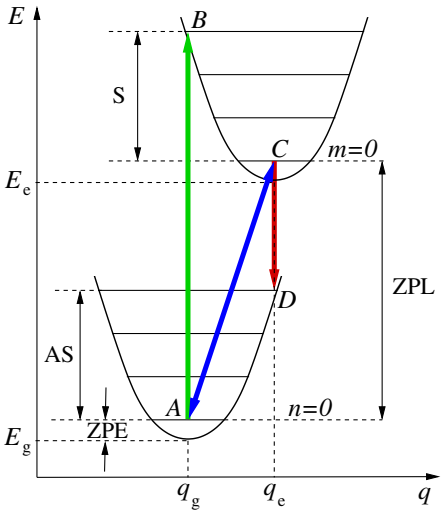

FIG. 2 (color online). The energy (E) vs configuration coordinate (q) diagram for the excitation process of a defect in the Franck-Condon approximation: E_g, E_e are the minima in the quasiparabolic potential energy surfaces of the defect in the ground and excited states, respectively, and q_g, q_e the corresponding coordinates. ZPE is the zero-point energy (indicated only for the ground state). The energy ladders show the phonon energies with the phonon ground states at $n = 0$ (ground state of the defect) and $m = 0$ (excited state). At elevated temperatures the high-energy phonon states can be occupied by inducing transition $A \rightarrow B$ (vertical absorption, green arrow), and $C \rightarrow D$ (vertical emission, red arrow). Transition $A \leftrightarrow C$ corresponds to the zero-phonon line (ZPL, blue double arrow) both in absorption and emission. The energy of the Stokes shift (S) and anti-Stokes shift (AS) are also shown.

The Franck-Condon approximation is commonly used to interpret the excitation spectrum, that is, assuming that the electronic transition is very fast compared with the motion of nuclei in the lattice. In addition to the Franck-Condon assumption, three other approximations are commonly assumed (see Fig. 2). The first is that each lattice vibration mode is well described by a quantum harmonic oscillator, as implied by the quasiparabolic shape of the potential wells, and almost constant energy spacing between phonon energy levels. The second, called the low-temperature approximation, is that only the lowest (zero-point) lattice vibration is excited, implying that electronic transitions do not originate from any of the higher phonon levels. The third, called the linear-coupling approximation, is that the interaction between the defect and the lattice is the same in both the ground and the excited states; this implies two equally shaped parabolic potentials and equally spaced phonon energy levels in both the ground and excited states. The detected phonon peaks in the spectrum may be associated with the $m = 1, 2, \ldots$ and $n = 1, 2, \ldots$ quanta of a characteristic phonon mode in absorption and emission. The highest intensity in the phonon side band at low temperatures corresponds to the excitations where the geometry does not change, that is, the vertical absorption and emission [19]. This way the Stokes and anti-Stokes shifts are determined, which reveal the relaxation energy of the atoms due to the electronic excitation (see Fig. 2). In the linear-coupling approximation the Stokes and anti-Stokes shifts would have the same value but experimental measurements indicate a difference of about 0.05 eV (see Table I and related discussion).

Another complication in understanding the excitation and deexcitation processes arises from a recent measurement [10] of the highest emission intensity in the phonon sideband at ≈ 1.880 eV. In this measurement, the second peak at 1.820 eV is clearly visible but the third at 1.760 eV is almost missing [10]. This measurement was carried out at 10 K. This is puzzling since at higher temperature (for instance, at liquid-nitrogen temperature, 77 K, where

TABLE I. The calculated vertical absorption ($A \rightarrow B$) and vertical emission energies ($C \rightarrow D$), and the zero-phonon line (ZPL) obtained with the PBE and HSE06 functionals, compared to measured values from Ref. [2]. The Stokes shift (S) between the vertical absorption and the ZPL, and the anti-Stokes-shift (AS) between the ZPL and the vertical emission are also given (all values in eV).

	ZPL	$A \rightarrow B$	S	$C \rightarrow D$	AS
PBE	1.706	1.910	0.204	1.534	0.172
HSE06	1.955	2.213	0.258	1.738	0.217
Exp. [2]	1.945	2.180	0.235	1.760	0.185

earlier experiments were conducted [2]), higher-energy phonon states can be occupied resulting in larger vertical emission energy, the opposite of what was found in the recent measurements [10]. We note that in the latter, low-temperature (10 K) experiment, a laser beam was focused with a 10 cm lens, increasing the energy density by a factor of 10^4. In fact, this experiment measured the ionization of $N - V^-$ defects from the ^3E excited state during the high intense excitation [10]. Assuming that all the usual approximations hold for this process, an anti-Stokes shift of 0.065 eV can be deduced [10] which clearly contradicts the results of earlier experiments [2]. This issue must be addressed and resolved in a full explanation of the process.

The standard method to investigate defect properties in solids is the application of DFT in a supercell geometry. While the ground-state charge and spin density can be obtained accurately using the local density approximation (LDA) for the exchange-correlation functional, or by other functionals that include density-gradient corrections (for example, the PBE functional [13]), the accurate calculation of the excitation energies is formally outside the scope of the ground-state Kohn-Sham DFT. For example, the LDA value for the zero-phonon line (ZPL) of the $N - V^-$ center is 1.71 eV [15] compared to the experimental 1.945 eV [2]. Ideally, for the calculation of the excitation energies, the Bethe-Salpeter equation should be solved, following a parameter-free self-consistent *GW* calculation [20], but this is computationally prohibitive for large supercells. Screened hybrid density functionals mix Hartree-Fock (HF) exchange with the PBE exchange within the Kohn-Sham formalism, but strictly speaking are out of the bounds of the original theory, mimicking the effect of a self-interaction correction. The 25% mixing parameter of the HSE06 hybrid functional, which is used here, was chosen to provide the best effect on calculated thermochemical data, while the only other parameter, a screening length of 4.81 Å, have been fixed empirically to fit the optical band gaps of 13 semiconductors by the (generalized) Kohn-Sham eigenvalue gap (with a mean absolute error of only 0.21 eV) [11,12]. It was shown that such hybrids reproduce not only the gap but also the whole excitation spectrum in a wide energy range for many semiconductors [21,22] and give better band lineups as well [23]. This gives hope for reproducing defect related excitations as well, as indeed it turns out to be the case here.

We employed two methods to calculate the excitation properties of the $N - V^-$ center in diamond: the traditional PBE functional and the HSE06 hybrid functional. First, the diamond primitive lattice was optimized, then a simple cubic 512-atom supercell was constructed. Finally, we placed the negatively charged nitrogen-vacancy defect in the supercell, and optimized the structure for each given electronic configuration. We employed the VASP5.1 code [24,25] to carry out these calculations with a plane-wave basis set (using an energy cutoff of 420 eV) and PAW-type potentials to model the atomic cores [26,27]. (For the optimization of the lattice constant we used a plane-wave cutoff energy of 840 eV and a $12 \times 12 \times 12$ Monkhorst-Pack k point set [28] for the primitive diamond lattice.) For the 512-atom supercell we used the Γ point that provides a well-converged charge density. We note here that all these calculations use the Born-Oppenheimer approximation that is valid at low temperatures.

The calculated lattice constant of diamond differs only slightly between the PBE (3.567 Å) and HSE06 (3.545 Å) approximations. However, while the PBE gap between the highest occupied end lowest unoccupied Kohn-Sham eigenvalues is only 4.16 eV [29], the generalized Kohn-Sham eigenvalues of HSE06 give 5.43 eV, very close to the experimentally observed 5.48 eV. As we will see, the defect excitation energy can be obtained by the HSE06 functional with similar accuracy.

The $^3A_2$ ground state of the $N - V^-$ center is obtained by spin polarized calculations both with the PBE and HSE06 functionals. The ^3E excited state is simply obtained by promoting one electron from the a_1 defect level to the e defect level in the band gap [14,15]. The total energy was minimized for both electronic configurations as a function of the coordinates of the nuclei, which allows us to determine the configuration coordinates of the ground state (q_g) and the excited state (q_e) of the defect. The corresponding energy minima in the calculations are shown as E_g and E_e in Fig. 2. The zero-point vibration states ($n = 0$ and $m = 0$) will raise these energies by a value of order a few tens meV, called zero-point energy (ZPE, shown in Fig. 2); for example, Davies and Hamer [2] deduced a ZPE value of ≈ 35 meV. We note that the difference between the ZPE values of E_g and E_e is expected to be even smaller, of order a few meV. The energy difference between the energy minima of E_g and E_e therefore gives a very good estimate of the ZPL ($A \rightarrow C$ transition; see Fig. 2). The transitions $A \rightarrow B$ and $C \rightarrow D$ are readily calculated by fixing the geometry at q_g and q_e, respectively, while varying the electronic configurations as explained above. We note that the error associated with the ZPE cannot be avoided in the calculated $A \rightarrow B$ and $C \rightarrow D$ transitions, which means that the values for these transitions are less accurate than for the ZPL. The calculated excitation energies (total energy differences between the ground and the excited state) using the PBE and HSE06 functionals are given in Table I.

The PBE functional gives too low values for the ZPL ($\approx$1.71 eV), so this gradient corrected functional does not improve the LDA value (1.71 eV [15]) at all. In contrast, the HSE06 functional gives an almost perfect value, the difference from experiment being smaller than 0.5%. Apparently, the HSE06 functional improves not just the band gap of the perfect semiconductor but the internal defect transition energy as well. The PBE functional does not improve the LDA values for the vertical absorption energy either, which is again too low by $\approx$0.3 eV. The HSE06 functional yields again an almost perfect value for

the energy of the vertical absorption compared to the experimental result (within 1.4%). The larger discrepancy for the $A \rightarrow B$ transition than for the ZPL may be attributed to the intrinsic ZPE error as explained above. We note that the calculated Stokes shift (the relaxation energy), is close to the experimental result from both the PBE and the HSE06 functionals. The reason is that any error inherent in the PBE functional is almost fully canceled, as the relaxation energy corresponds to the energy difference between two different atomic configurations with the same electronic configuration. The wave functions and the spin density obtained with the HSE06 functional are somewhat more localized than those obtained with the PBE functional. For example, the integrated spin density of the ^3E state in a 5^3 Å^3 cube centered at the vacant site containing the three carbon atoms and the nitrogen atom is 1.61 and 1.64 obtained in PBE and HSE06 calculations, respectively (see Fig. 1). This is an effect of the Hartree-Fock exchange, which usually gives more localized wave functions than the pure DFT-PBE. We note that similar localization can be observed upon a *GW* correction of the PBE states.

Having established the high level of accuracy of the HSE06 functional, we can address the issue of the vertical emission energy and the anti-Stokes shift. The value calculated with the PBE functional significantly differs from any experimental data. The HSE06 value (1.738 eV) is very close to the measurement of Davies and Hamer (1.760 eV) [2]. Since our calculations are valid at low temperature we assume that the low-temperature approximation beyond the Franck–Condon assumption holds for this transition. We conclude that the anti-Stokes shift is 0.185 eV at usual experimental conditions at low temperatures for the $N - V^-$ defect in diamond. For this defect the linear-coupling approximation does not hold. The difference between the Stokes and anti-Stoke shifts is $\approx (0.235 - 0.185)$ eV $= 0.050$ eV in experiment, which compares favorably to the HSE06 value $(0.258 - 0.217)$ eV $= 0.041$ eV. This indicates a somewhat different shape of the PES for the ground state and the excited state, thus different vibration modes.

The only remaining unresolved issue is the recent experiment suggesting a much lower anti-Stokes value of 0.065 eV [10]. We suggest that the high-energy-density excitation in this experiment resulted in local heating of the sample in the area where the laser beam was focused. The local heating of the sample will break the low-temperature approximation and will cause a shift in the occupation of the phonon states from $m = 0$ to $m = 2$. That may explain why the detected vertical emission energy is larger at 10 K (at high energy density) than at 77 K (at low energy density) excitation. Our results indicate that detailed analysis of the vibration modes of the ^3E excited state is important for a complete understanding of the radiative emission of the $N - V^-$ center; further experimental and theoretical efforts are needed in this direction.

A. G. acknowledges support from Hungarian OTKA No. K-67886, the Bolyai program from the Hungarian Academy of Sciences and the grant of SNIC001-08-175 from the Swedish National Supercomputer Center. P. D. acknowledges the grant HBC001 from HLRN supercomputer center. We thank Jeronimo Maze for fruitful discussions.

[1] L. du Preez, Ph.D. dissertation, University of Witwatersrand, 1965.
[2] G. Davies and M. F. Hamer, Proc. R. Soc. A **348**, 285 (1976).
[3] J. Wrachtrup, S. Y. Kilin, and A. P. Nizotsev, Opt. Spectrosc. **91**, 429 (2001).
[4] F. Jelezko *et al.*, Phys. Rev. Lett. **93**, 130501 (2004).
[5] R. J. Epstein, F. Mendoza, Y. K. Kato, and D. D. Awschalom, Nature Phys. **1**, 94 (2005).
[6] R. Hanson, F. M. Mendoza, R. J. Epstein, and D. D. Awschalom, Phys. Rev. Lett. **97**, 087601 (2006).
[7] L. Childress *et al.*, Science **314**, 281 (2006).
[8] M. V. Gurudev Dutt *et al.*, Science **316**, 1312 (2007).
[9] R. Hanson *et al.*, Science **320**, 352 (2008).
[10] N. B. Manson and J. P. Harrison, Diam. Relat. Mater. **14**, 1705 (2005).
[11] J. Heyd, G. E. Scuseria, and M. Ernzerhof, J. Chem. Phys. **118**, 8207 (2003).
[12] A. V. Krukau, O. A. Vydrov, A. F. Izmaylov, and G. E. Scuseria, J. Chem. Phys. **125**, 224106 (2006).
[13] J. P. Perdew, K. Burke, and M. Ernzerhof, Phys. Rev. Lett. **77**, 3865 (1996).
[14] J. P. Goss *et al.*, Phys. Rev. Lett. **77**, 3041 (1996).
[15] A. Gali, M. Fyta, and E. Kaxiras, Phys. Rev. B **77**, 155206 (2008).
[16] J. A. Larsson and P. Delaney, Phys. Rev. B **77**, 165201 (2008).
[17] F. M. Hossain, M. W. Doherty, H. F. Wilson, and L. C. L. Hollenberg, Phys. Rev. Lett. **101**, 226403 (2008).
[18] A. Gali and E. Kaxiras (unpublished).
[19] K. Huang and A. Rhys, Proc. R. Soc. A **204**, 406 (1950).
[20] L. Hedin and S. Lundqvist, in *Solid State Physics*, edited by H. Ehrenreich, F. Seitz, and D. Turnbull (Academic, New York, 1969), Vol. 23.
[21] M. Marsman, J. Paier, A. Stroppa, and G. Kresse, J. Phys. Condens. Matter **20**, 064201 (2008).
[22] J. Paier, M. Marsman, and G. Kresse, Phys. Rev. B **78**, 121201 (2008).
[23] A. Alkauskas, P. Broqvist, F. Devynck, and A. Pasquarello, Phys. Rev. Lett. **101**, 106802 (2008).
[24] G. Kresse and J. Furthmüller, Phys. Rev. B **54**, 11 169 (1996).
[25] J. Paier *et al.*, J. Chem. Phys. **124**, 154709 (2006).
[26] P. E. Blöchl, Phys. Rev. B **50**, 17 953 (1994).
[27] G. Kresse and D. Joubert, Phys. Rev. B **59**, 1758 (1999).
[28] H. J. Monkhorst and J. K. Pack, Phys. Rev. B **13**, 5188 (1976).
[29] The Kohn-Sham gap differs from the observed one by the value of the derivative discontinuity; see J. P. Perdew and M. Levy, Phys. Rev. Lett. **51**, 1884 (1983).